BJR

Received: 1 July 2013 | Revised: 31 July 2013 | Accepted: 3 September 2013

doi: 10.1259/bjr.20130398

Cite this article as:
Kok HK, Fitzgerald L, Campbell N, Lyburn ID, Munk PL, Buckley O, et al. Multimodality imaging features of hereditary multiple exostoses. Br J Radiol 2013;86:20130398.

PICTORIAL REVIEW

Multimodality imaging features of hereditary multiple exostoses

[1]H K KOK, MRCPI, MRCP (UK), [1]L FITZGERALD, MB BCh, [1]N CAMPBELL, MRCSI, FFRRCSI, [2]I D LYBURN, MRCP (UK), FRCR, [3]P L MUNK, MD, FRCPC, [1]O BUCKLEY, MRCPI, FFRRCSI and [1]W C TORREGGIANI, FRCR, FFRRCSI

[1]Department of Radiology, Tallaght Hospital, Dublin, Ireland
[2]Department of Radiology, Cheltenham General Hospital, Cheltenham, UK
[3]Department of Radiology, Vancouver General Hospital, BC, Canada

Address correspondence to: Dr Hong Kuan Kok
E-mail: *terrykok@gmail.com*

ABSTRACT

Hereditary multiple exostoses (HME) or diaphyseal aclasis is an inherited disorder characterised by the formation of multiple osteochondromas, which are cartilage-capped osseous outgrowths, and the development of associated osseous deformities. Individuals with HME may be asymptomatic or develop clinical symptoms, which prompt imaging studies. Different modalities ranging from plain radiographs to cross-sectional and nuclear medicine imaging studies can be helpful in the diagnosis and detection of complications in HME, including chondrosarcomatous transformation. We review the role and imaging features of these different modalities in HME.

Hereditary multiple exostoses (HME), also known as diaphyseal aclasis, is an autosomal dominant condition characterised by the presence of multiple oesteochondromas or exostoses with associated remodelling deformities in bones. Osteochondromas are cartilage-capped bony outgrowths, which typically develop around the metaphysis of long bones and may vary in size, morphology (being sessile or pedunculated) and number in affected individuals. Genetic mutations affecting the *EXT* genes on chromosomes 8q24 (*EXT1*), 11p11-13 (*EXT2*) and 19p (*EXT3*) that encode glycosyltransferase enzymes involved in the synthesis of heparan sulphate proteoglycans are thought to cause HME [1,2]. The most common clinical symptom is the presence of painless, single or multiple, hard exophytic masses near the joints of long bones, which may be associated with bony deformities [3]. Exostoses are usually not present at birth but become evident between the age of 2 and 10 years, with a diagnosis established during the first decade in the lives of >80% of individuals with HME [4]. The exostoses usually exhibit no further growth after closure of the growth plate unless complications develop.

IMAGING FEATURES

Exostoses may be unilateral or, more commonly, bilateral and may involve any bone in the body except the calvarium [5]. The common sites of involvement include the distal femur, proximal tibia, wrist and hands, humerus, ankle, pelvis and ribs [6,7]. Plain radiographs of the affected region remain the mainstay of radiological diagnosis in HME helping to readily identify exostoses and bony deformities. However, other imaging modalities, such as ultrasound, CT, MRI, radionuclide bone scintigraphy and positron emission tomography are useful in the detection of HME.

Characteristic long bone deformities are seen in HME, and these occur because of the disruption of normal epiphyseal growth plate cartilage with abnormal bone remodeling, particularly in the diametaphyseal region. About one-third of patients demonstrate a characteristic "bayonet hand" or pseudo-Madelung deformity in the upper limbs because of foreshortening of the ulna in relation to the radius (Figure 1) [7]. In the lower limbs, osteochondromas are usually found around the knee joint in the distal femur or proximal tibia and fibula with a widening of the distal femoral diametaphyseal junction, producing an Erlenmeyer flask deformity (Figures 2–4). Valgus deformity of the femur (coxa valga), producing a more vertical orientation of the femoral neck (Figure 5), limb length discrepancies and short stature can also be seen.

COMPLICATIONS IN HEREDITARY MULTIPLE EXOSTOSES

Malignant transformation with the development of a chondrosarcoma in the cartilage cap of an osteochondroma is the

Figure 1. Forearm radiographs showing a pseudo-Madelung deformity as a result of ulnar foreshortening with bowing of the radius.

most feared complication of HME. This is heralded clinically by pain and a rapid increase in the size of a previously asymptomatic osteochondroma (Figure 6) [8]. Malignant transformation has an estimated prevalence of 1% in patients with solitary osteochondroma but is much higher (up to 25%) in patients with HME [4,7]. The thickness of the cartilage cap of an osteochondroma is used as an indicator of malignant transformation and can be accurately measured using ultrasound (Figure 3) or MRI (Figure 7) [5,9]. A cartilage cap thickness of >2 cm in a skeletally mature patient is highly suspicious for malignant transformation, although the cartilage cap thickness varies depending on skeletal maturity, being thicker (up to 3 cm) in the paediatric population. Cartilage cap thickness should be measured in a standardised manner from the osseous interface of the osteochondroma stalk to the outermost edge of the cartilage cap at its thickest portion, excluding crevasses. This measurement technique has been reported to have a sensitivity and specificity of >95% in the detection of secondary chondrosarcomas using a 2-cm threshold [10]. Positron emission tomography with 18-fludeoxyglucose has also been reported to be accurate in the detection of cartilage dedifferentiation and malignant transformation [11,12] (Figures 8 and 9). However, single standing planar bone scintigraphy has no value in distinguishing benign osteochondromas from malignant chondrosarcomas [13].

Figure 2. Knee radiographs of a young patient with hereditary multiple exostoses showing multiple exostoses in the distal femur and proximal tibia and fibula, which typically point away from the joint. There is an associated widening of the diametaphysis resulting in an Erlenmeyer flask deformity.

In addition to the osseous deformities described earlier, additional complications in HME are mostly related to the presence of exostoses and include fractures from local trauma, vascular compromise, impingement on nerves and tendons and overlying bursa formation [3,4]. Vascular complications occur as a result of vessel compression or displacement and may result in stenosis with subsequent occlusion or pseudoaneurysm formation (Figure 10). Similarly, neurological complications are because of the direct impingement on adjacent nerves. Spinal cord and cranial nerve impingements have been described, usually arising from ribs, vertebral or skull base osteochondromas [14,15]. More common is a peripheral nerve entrapment neuropathy, which frequently involves the radial and peroneal nerves [16,17]. Bursa formation is most frequently seen in the scapula, hip and shoulder and is the result of repetitive mechanical friction between exostoses and soft tissue [5]. Inflammation or bursitis may lead to further clinical symptoms specific to the site of involvement (Figure 11). Additional rare but recognised complications include urinary and intestinal obstruction, dysphagia secondary to ventral cervical exostoses, spontaneous haemothorax secondary to rib exostoses and interference with normal vaginal deliveries, thereby requiring caesarean section [4].

CONCLUSIONS

HME can be diagnosed based on the typical radiographic findings of multiple exostoses with associated skeletal deformities. Individuals with HME who develop symptoms of increasing swelling or pain at an affected body site require careful clinical work-up and imaging.

Figure 3. (a) Anteroposterior and (b) lateral radiographs demonstrating an exostosis in the proximal left fibula. The cartilage cap is usually not seen on radiographs but can be detected using (c) ultrasound or MRI. A thickness of >2 cm in a skeletally mature patient may be suspected for transformation to a chondrosarcoma.

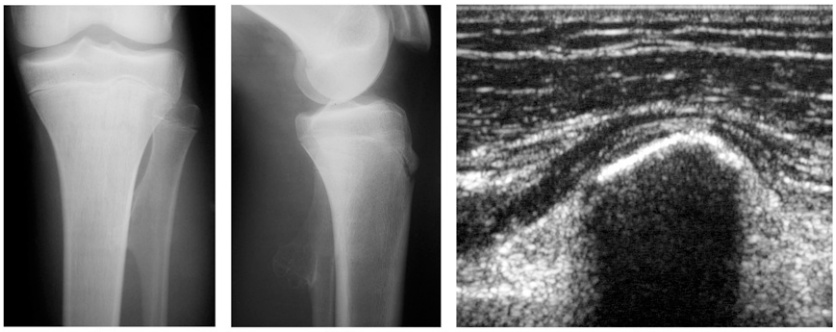

Figure 4. Exostosis (black arrow) in the proximal right tibia causing compression and lateral bowing of the adjacent fibula.

Figure 5. Coxa valga in a patient with hereditary multiple exostoses showing bilaterally increased femoral angles resulting in a more vertical orientation of the femoral neck.

Figure 6. Frontal knee radiographs in a 15-year-old male patient (a) at the time of diagnosis of hereditary multiple exostoses demonstrating an exostosis at the distal right femur. (b) Radiograph taken after 3 years because of symptoms at the site of exostosis, showing interval growth of the exostosis after skeletal maturity. Ongoing growth raises suspicion of malignant transformation, and further evaluation using MRI should be performed.

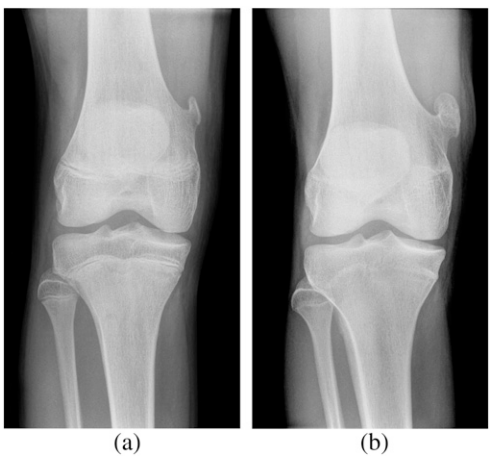

Figure 7. Male patient with known hereditary multiple exostoses presenting with left deltoid pain and swelling. (a) Radiograph of the left humerus demonstrating two exostoses in the proximal diaphyseal region. Prominent ring and arc calcification and thickening of the cartilage cap is seen in the lateral exostosis. (b) Coronal CT confirms thickening of the cartilage cap suggestive of malignant chondrosarcomatous transformation. (c) Axial T_2 weighted MRI showing a hyperintense thick multilobulated lesion in the proximal humerus because of an enlargement of the hyaline cartilage component that is highly suggestive of malignant transformation. (d) Radionuclide bone scintigram showing high radiotracer uptake in the proximal lateral left humerus corresponding to the site of malignant transformation.

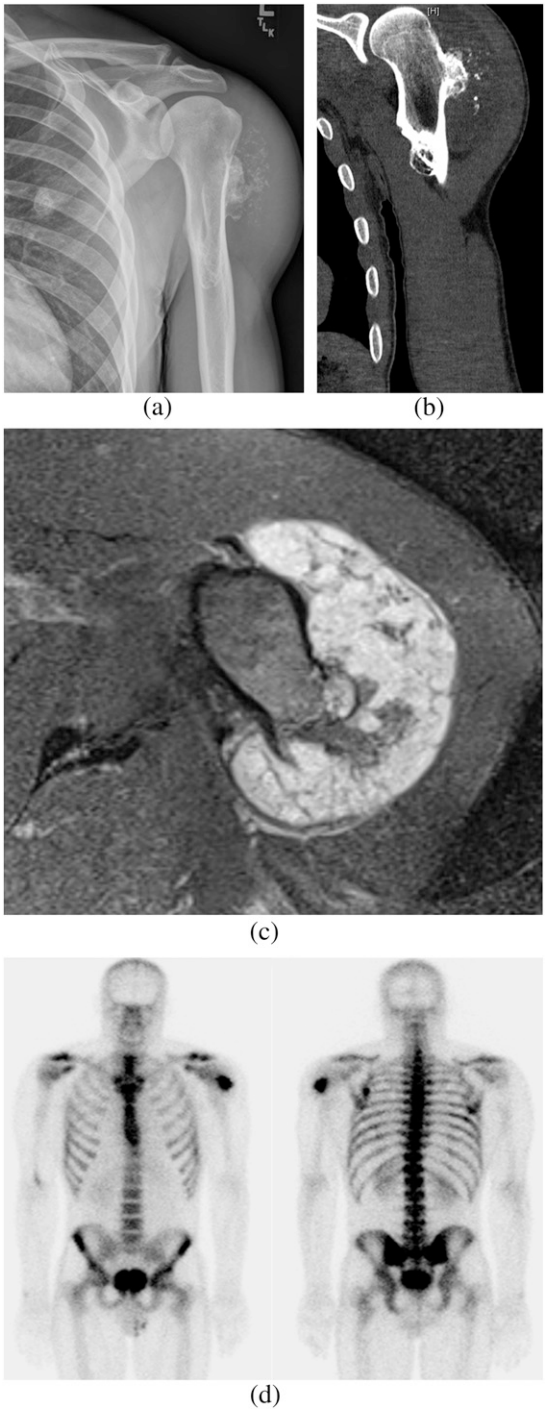

(a) (b) (c) (d)

Figure 8. (a) Large right scapular osteochondroma in a patient with hereditary multiple exostoses presenting with increasing pain and swelling (black arrow) showing a chondroid matrix throughout the lesion. (b) Fused axial 18-fludeoxyglucose (^{18}FDG)-positron emission tomography-CT image demonstrating ^{18}FDG-avid hypermetabolic foci in the right scapula concerning for chondrosarcoma.

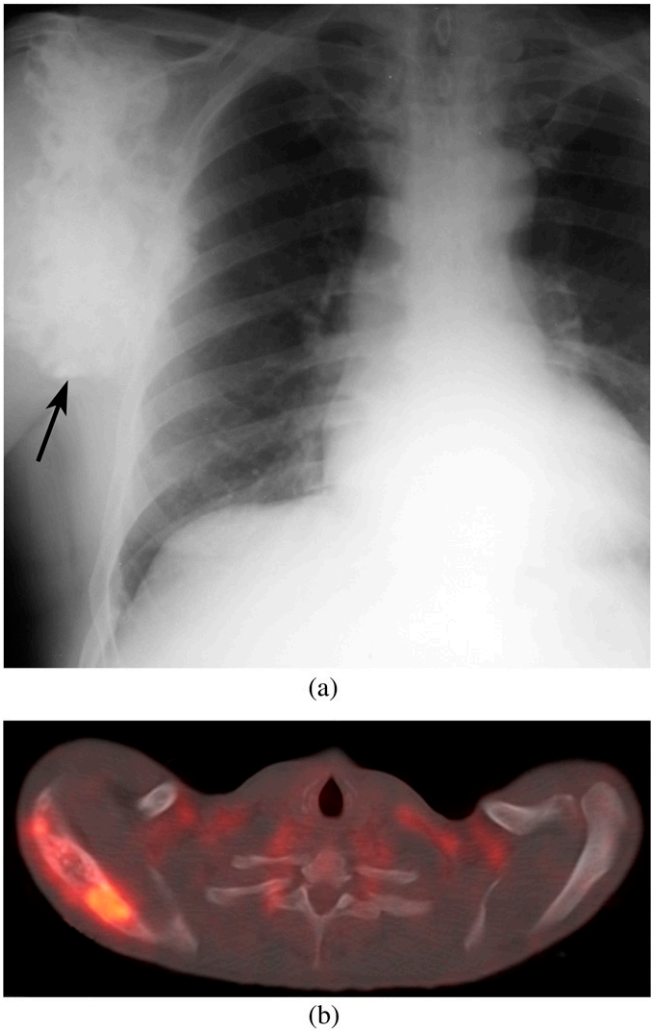

(a) (b)

Figure 9. (a) Axial CT, (b) 18-fludeoxyglucose (^{18}FDG)-positron emission tomography (PET) and (c) fused ^{18}FDG-PET-CT images through the pelvis, in a patient with hereditary multiple exostoses presenting with worsening right hip pain. The right iliac bone is involved by an aggressive process with avid ^{18}FDG uptake compatible with a chondrosarcoma.

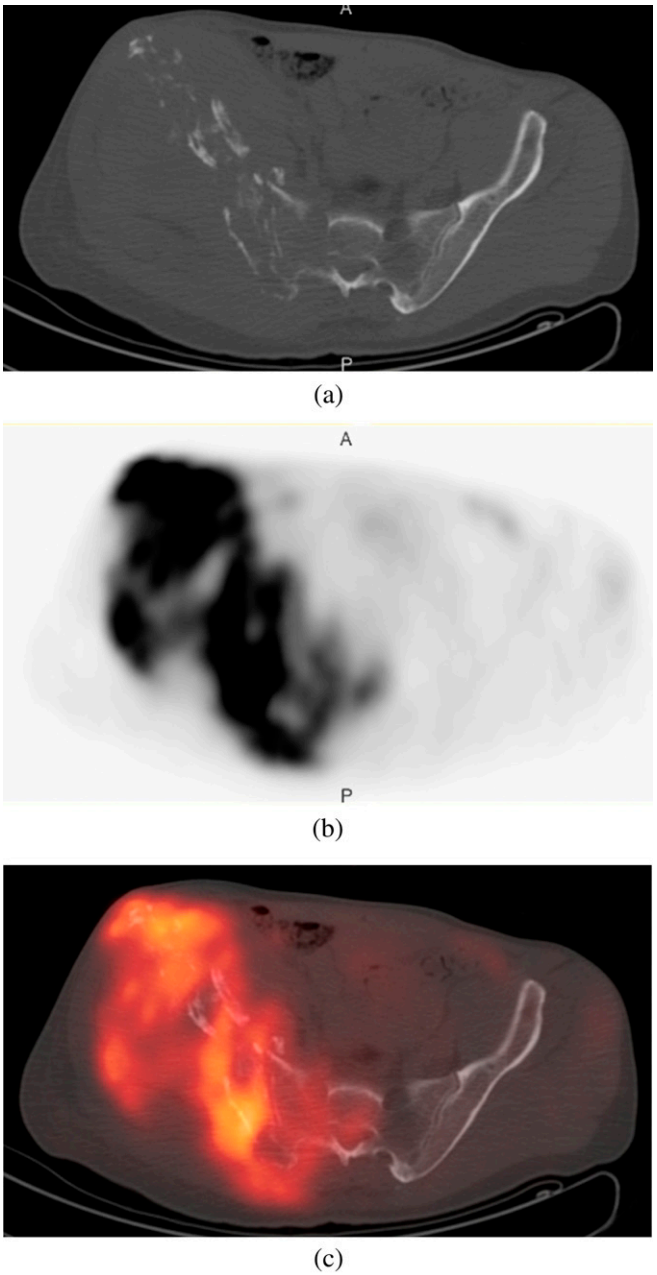

Figure 10. Axial CT thorax image showing an exostosis involving the first right rib adjacent to the brachiocephalic artery. Direct compression or entrapment of neighbouring vessels can result in vascular compromise and distal ischaemic symptoms.

Figure 11. Axial T_2 weighted MRI of the distal femur in a patient with pain and swelling in the thigh. A high-signal fluid collection is seen between the exostosis and vastus lateralis muscle (white arrow), where associated soft-tissue oedema is present, consistent with bursa formation and inflammation (bursitis).

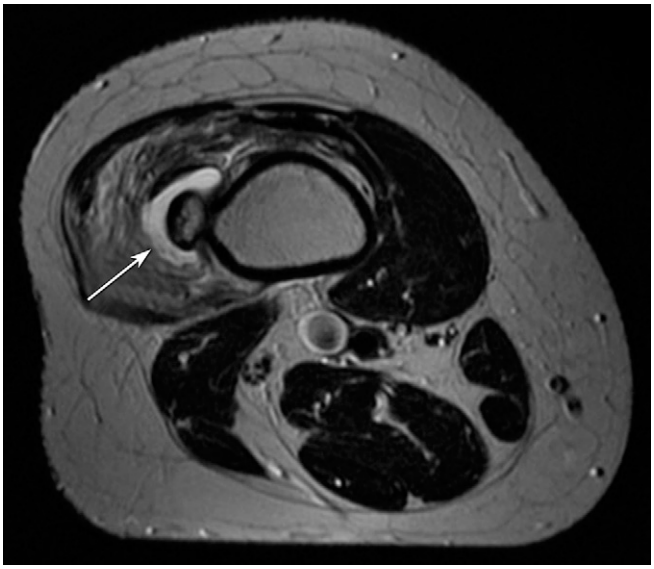

REFERENCES

1. Francannet C, Cohen-Tanugi A, Le Merrer M, Munnich A, Bonaventure J, Legeai-Mallet L. Genotype-phenotype correlation in hereditary multiple exostoses. J Med Genet 2001;38:430–4.
2. Porter DE, Lonie L, Fraser M, Dobson-Stone C, Porter JR, Monaco AP, et al. Severity of disease and risk of malignant change in hereditary multiple exostoses. A genotype-phenotype study. J Bone Joint Surg Br 2004;86:1041–6.
3. Karasick D, Schweitzer ME, Eschelman DJ. Symptomatic osteochondromas: imaging features. AJR Am J Roentgenol 1997;168:1507–12. doi: 10.2214/ajr.168.6.9168715

4. Stieber JR, Dormans JP. Manifestations of hereditary multiple exostoses. J Am Acad Orthop Surg 2005;13:110–20.
5. Murphey MD, Choi JJ, Kransdorf MJ, Flemming DJ, Gannon FH. Imaging of osteochondroma: variants and complications with radiologic-pathologic correlation. Radiographics 2000;20:1407–34.
6. Shapiro F, Simon S, Glimcher MJ. Hereditary multiple exostoses. Anthropometric, roentgenographic, and clinical aspects. J Bone Joint Surg Am 1979;61: 815–24.
7. Vanhoenacker FM, Van Hul W, Wuyts W, Willems PJ, De Schepper AM. Hereditary multiple exostoses: from genetics to clinical syndrome and complications. Eur J Radiol 2001;40: 208–17.
8. Shah ZK, Peh WC, Wong Y, Shek TW, Davies AM. Sarcomatous transformation in diaphyseal aclasis. Australas Radiol 2007;51:110–9. doi: 10.1111/j.1440-1673.2007.01679.x
9. Malghem J, Vande Berg B, Noël H, Maldague B. Benign osteochondromas and exostotic chondrosarcomas: evaluation of cartilage cap thickness by ultrasound. Skeletal Radiol 1992; 21:33–7.
10. Bernard SA, Murphey MD, Flemming DJ, Kransdorf MJ. Improved differentiation of benign osteochondromas from secondary chondrosarcomas with standardized measurement of cartilage cap at CT and MR imaging. Radiology 2010;255:857–65. doi: 10.1148/radiol.10082120
11. Feldman F, Van Heertum R, Saxena C, Parisien M. 18FDG-PET applications for cartilage neoplasms. Skeletal Radiol 2005;34: 367–74. doi: 10.1007/s00256-005-0894-y
12. Purandare NC, Rangarajan V, Agarwal M, Sharma AR, Shah S, Arora A, et al. Integrated PET/CT in evaluating sarcomatous transformation in osteochondromas. Clin Nucl Med 2009;34:350–4. doi: 10.1097/RLU.0b013e3181a34525
13. Hendel HW, Daugaard S, Kjaer A. Utility of planar bone scintigraphy to distinguish benign osteochondromas from malignant chondrosarcomas. Clin Nucl Med 2002; 27:622–4. doi: 10.1097/01RLU.0000023879.58875.B1
14. Jackson A, Hughes D, St Clair Forbes W, Stewart G, Cummings WJ, Reid H. A case of osteochondroma of the cervical spine. Skeletal Radiol 1995;24:235–7.
15. Sato K, Kodera T, Kitai R, Kubota T. Osteochondroma of the skull base: MRI and histological correlation. Neuroradiology 1996;38:41–3.
16. Cardelia JM, Dormans JP, Drummond DS, Davidson RS, Duhaime C, Sutton L. Proximal fibular osteochondroma with associated peroneal nerve palsy: a review of six cases. J Pediatr Orthop 1995;15:574–7.
17. Coenen L, Biltjes I. High radial nerve palsy caused by a humeral exostosis: a case report. J Hand Surg Am 1992;17:668–9.